The FERRUM project: experimental lifetimes of highly excited FeII 3d(6)4p levels and transition probabilities

Sikstrom, C. M; Schultz-Johanning, M; Kock, M; Li, Z. S; Nilsson, H; Johansson, S; Lundberg, Hans; Raassen, A. J. J

Published in:
Journal of Physics B: Atomic, Molecular and Optical Physics

DOI:
10.1088/0953-4075/32/24/306

1999

The FERRUM project: experimental lifetimes of highly excited Fe II $3d^6 4p$ levels and transition probabilities

1999 J. Phys. B: At. Mol. Opt. Phys. 32 5687

(http://iopscience.iop.org/0953-4075/32/24/306)

J. Phys. B: At. Mol. Opt. Phys. **32** (1999) 5687–5698. Printed in the UK PII: S0953-4075(99)05245-1

The FERRUM project: experimental lifetimes of highly excited Fe II $3d^6 4p$ levels and transition probabilities

C M Sikström†, M Schultz-Johanning‡, M Kock‡, Z-S Li§, H Nilsson†, S Johansson†, H Lundberg§ and A J J Raassen‖

† Atomic Spectroscopy, Department of Physics, PO Box 118, S-221 00 Lund, Sweden
‡ Institut für Atom- und Molekülphysik, Abt. Plasmaphysik, Universität Hannover, Callinstr. 38, D-30167 Hannover, Germany
§ Department of Physics, Lund Institute of Technology, PO Box 118, S-221 00 Lund, Sweden
‖ Astronomical Institute 'Anton Pannekoek', University of Amsterdam, Kruislaan 403, 1098 SJ, Amsterdam, The Netherlands

Received 14 July 1999

Abstract. We report on measurements of radiative lifetimes in singly ionized iron of six $3d^6 4p$ levels between 61 512 and 64 041 cm^{-1}, using time-resolved laser-induced fluorescence. Absolute oscillator strengths of 18 Fe II lines in the wavelength range from 2350 to 2800 Å have been obtained by measuring branching fractions for the lines from two Fe II levels with a Fourier-transform spectrometer. The uncertainty in the lifetimes is between 8% and 13%, whereas the uncertainty of the f-values varies between 9% and 19%. A comparison with several previously published values is given.

1. Introduction

Evaluation and extraction of information from the line spectrum of an absorbing radiating plasma, e.g. the outer atmosphere of a star, requires knowledge about specific atomic parameters, such as the wavelength, oscillator strength and damping constants. These parameters are linked to the position, depth and shape of the spectral lines. Thus, accurate wavelengths are needed for positive line identifications, giving a qualitative measure of the chemical content of a stellar atmosphere, whereas accurate oscillator strengths (f-values) are required for a quantitative determination of the relative abundances of the elements. Knowledge about the relative abundances is an important ingredient in studies of galactic stellar evolution. The shape of spectral lines may provide information about the physical conditions of the radiating plasma, but the analysis of the line profile must include the possible influence of the Zeeman effect, hyperfine structure and isotope shifts.

Studies of chemical abundances in stellar atmospheres are based on a bulk of calculated values and a limited number of experimental values of oscillator strengths for each element and ion. There are more experimental data available for the lighter elements than for the heavier ones. The theoretical f-values seldom have an estimate of their accuracy, whereas recent experimental data may have uncertainties in the range 1–50%. The most accurate f-values are often associated with the most prominent lines, e.g. the resonance lines, which are often saturated in stellar spectra and less usable in quantitative abundance analyses. The contribution of lines to a stellar spectrum from a specific element depends on its relative abundance and the energy level structure of the particular ions present. Fe II is perhaps the most dominant

0953-4075/99/245687+12$30.00

contributor to the absorption line spectra of stellar photospheres at moderate temperatures and also to the emission line spectra of extended stellar atmospheres and surroundings. Fe II also plays an important role in the understanding of the spectra of quasars and active galactic nuclei (Verner *et al* 1999).

In a newly started international collaboration, the FERRUM project (project leader: S Johansson, Lund University), we intend to extend and improve the database of oscillator strengths for Fe II by combining radiative lifetimes and experimental as well as theoretical branching fractions. The information about f-values indirectly present in high-quality stellar spectra (Brandt *et al* 1999, Leckrone *et al* 1999) will also be utilized in the FERRUM project. The lifetimes are measured by laser-induced fluorescence (LIF) techniques at the Lund Laser Centre (LLC) and the branching ratios by calibrated emission line spectra, which are recorded using a Fourier-transform spectrometer (FTS) at the Division for Atomic Spectroscopy (both facilities are at Lund University). In a previous paper (Li *et al* 1999a, hereafter called paper 1) we have described the technique of the lifetime measurements.

Previous experimental f-value data for Fe II based on LIF lifetimes and experimental branching fractions comprise levels of only the lowest odd-parity subconfiguration $3d^6(^5D)4p$ (see references in paper 1 and Schnabel *et al* 1999). Thus, the lower energy level of the Fe II lines used for accurate abundance studies has an excitation energy of less than 4 eV. To broaden the range of excitation potentials a new step was taken in paper 1, where two levels of intermediate excitation (about 7.5 eV) were studied. The aim of the FERRUM project is to obtain accurate f-values for absorption lines of Fe II in the optical and ultraviolet (UV) wavelength regions originating from levels from an extended region of excitation energies, 0–10 eV.

In the present paper we present radiative lifetimes of six Fe II levels from the $3d^6(^3H)4p$ and $3d^6(^3F)4p$ subconfigurations, having excitation energies of about 7.5 eV. The levels have been excited from a metastable state below 2.0 eV. Two of the levels, $3d^6(^3H)4p\ z\ ^4I_{9/2}$ and $z\ ^2I_{11/2}$ have all their strong decay channels above 1850 Å, and experimental branching ratios have been determined for the strongest transitions from these levels. By combining the lifetimes and branching fractions experimental oscillator strengths have been derived for 18 Fe II lines in the 2000–3000 Å region.

2. Atomic structure of Fe II

In order to relate the energy levels included in the present measurements to the term diagram of Fe II we give a brief overview of the complex atomic structure of Fe II. There are two main systems of configurations: $3d^6nl$, the singly excited (SE) system, and $3d^54snl$, the doubly excited (DE) system. The SE system has a somewhat higher binding energy than the DE system. The SE system is based on 16 parent terms—16 LS terms of the $3d^6$ ground configuration of Fe III. Each $3d^6nl$ configuration can therefore be split up in 16 subconfigurations $3d^6(^ML)nl$ based on the different parent terms ^ML. This is illustrated in figure 1, where each box represents a subconfiguration. All subconfigurations belonging to a particular parent term are displayed along a vertical line. All subconfigurations belonging to the same configuration can be connected horizontally, and they follow the pattern of the parent configuration $3d^6$ in Fe III, as illustrated in the figure. Because of the Pauli principle the $3d^7$ configuration does not give a full set of LS terms, and the resulting terms cannot be traced to a particular parent. Therefore, the whole $3d^7$ configuration has been represented by one box in figure 1.

The ground term of Fe II, $3d^6(^5D)4s\ a\ ^6D$, belongs to the SE system and is based on the ground term $3d^6\ ^5D$ in Fe III. The resonance lines arise from 4s–4p combinations with the $3d^6(^5D)4p$ levels, and in figure 1 we can see that the distance is about 40 000 cm^{-1}. This is

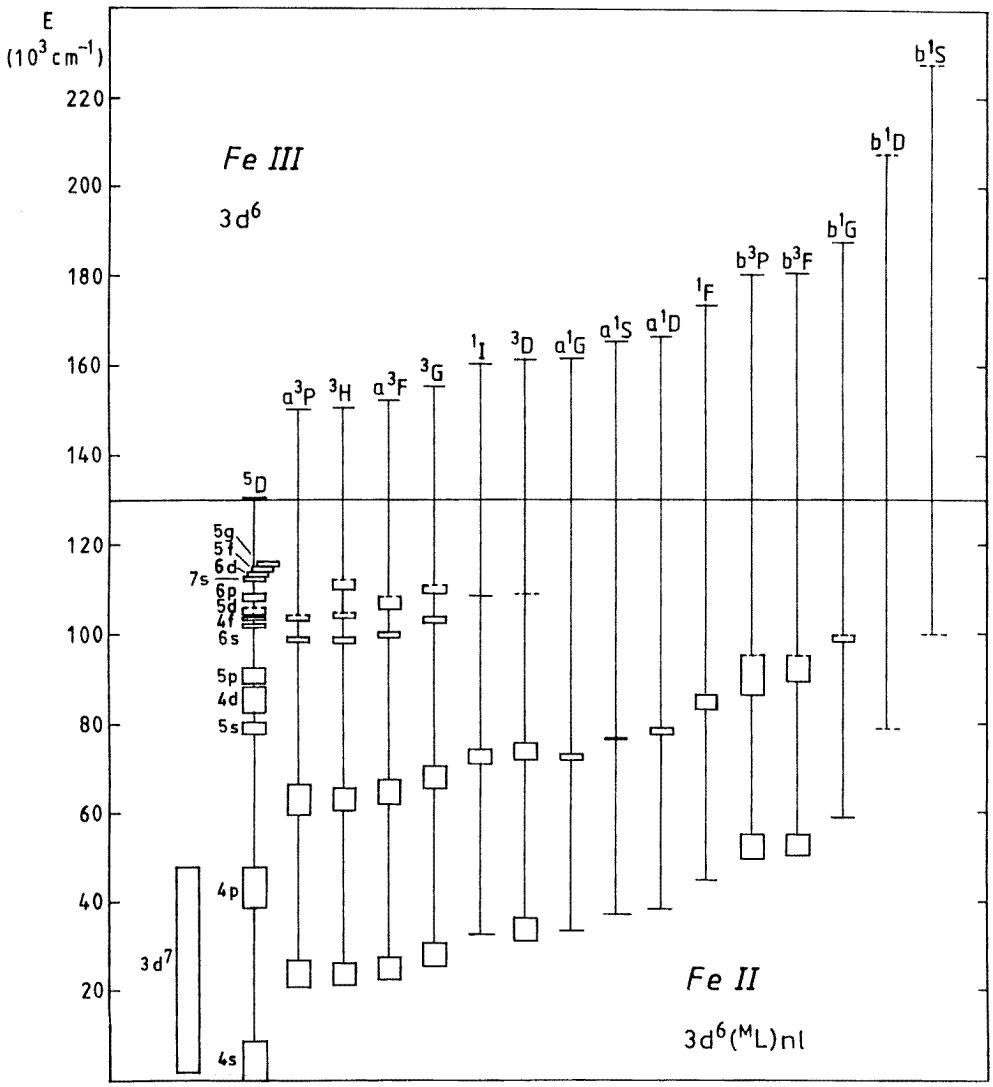

Figure 1. Illustration of the complex parent term structure of Fe II.

the distance between the two 4s and 4p boxes along any vertical line, indicating that all strong 4s–4p lines fall in about the same wavelength region, 2300–2700 Å.

Most experimental work on LIF lifetimes has hitherto been focused on the lowest 4p box (the 25 levels of the $3d^6(^5D)4p$ *LS* terms $z\,^6F$, D, P and $z\,^4F$, D, P) mainly due to the problem of wavelength limitations in the laser excitation of higher terms. There are two possibilities to reach higher terms: to start from low levels and increase the laser frequency or to excite the levels from metastable states. In the FERRUM project we have chosen a compromise to reach higher 4p states, and in figure 2 we show the excitation and de-excitation of one of the levels studied in the present paper ($3d^6(a\,^3H)4p\,z\,^4I_{9/2}$). We utilize the possibility to start from a metastable $3d^7$ level and excite the upper level via a 3d–4p transition. Some experimental problems arise in the lifetime measurements when starting the excitation from high metastable

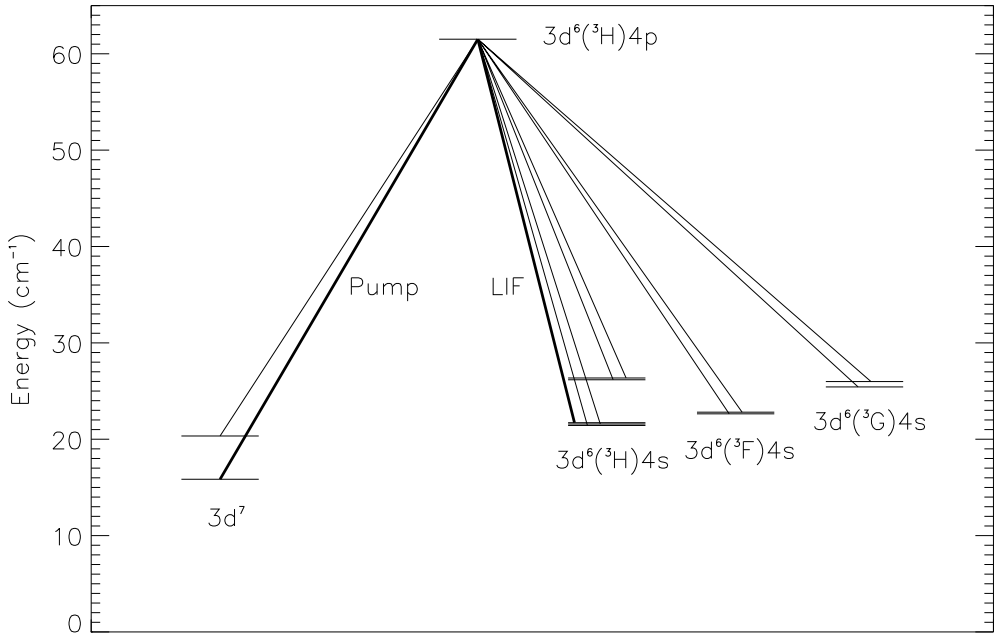

Figure 2. Excitation and de-excitation of the level $3d^6$(a ^{3}H)4p z $^4I^o_{9/2}$. The thick lines mark the pump channel and the fluorescence transition used in the lifetime measurement of the upper level.

states as discussed at the end of section 3. Wavelength limitations of the FTS cause problems in branching ratio measurements of levels having strong 3d–4p transitions below 1800 Å. On the other hand, for high 4p levels having very weak branches at short wavelengths, the BFs including high metastable states should be more reliable due to fewer problems with self-absorption in the light source. We have therefore concentrated our work on such levels in the present paper.

3. Measurements of radiative lifetimes

The Fe II lifetimes presented in table 1 were measured using the method of time-resolved LIF. The ion source used in the experiment was an ablation-produced plasma using a pulsed Nd:YAG-laser focused onto a rotating iron target. The pulse energy and focus can be adjusted to provide appropriate plasma conditions. An illustration of the experimental set-up can be found in figure 3.

The laser used to pump the dye laser of the excitation pulse system was a seeder injected Nd:YAG laser (Continuum NY 82-10), giving pulses with a duration of roughly 10 ns. The pulse from the Nd:YAG was frequency doubled to give green light at 532 nm. The temporal shape of the Nd:YAG output was compressed by means of stimulated Brillouin scattering (SBS). The compressor consists of a 1.5 m long glass tube (the length of the tube should be matched to half the length of the laser pulse) filled with water, which is used as the active substance. A short-focus lens near the end of the tube focuses the laser beam to a small point, where the SBS takes place and a mirror is formed. The mirror then travels back with the reflected pulse, compressing the pulse length from 10 ns to <1 ns (FWHM). The pulse

Table 1. Radiative lifetimes of Fe II levels excited from the metastable $a\,^2G_{9/2}$ level (15 844.65 cm^{-1}). Det. λ is the wavelength at which the LIF was detected.

					Lifetime (ns)	
Configuration	Term	J	E (cm^{-1})	Det. λ (Å)	This work	SW[a]
$3d^6(a\,^3H)4p$	$z\,^4I^o$	9/2	61 512.63	2511.760	3.5 ± 0.3	
$3d^6(a\,^3F)4p$	$y\,^4F^o$	7/2	62 065.52	2546.670	3.5 ± 0.3	
$3d^6(a\,^3H)4p$	$z\,^2I^o$	11/2	62 662.24	2753.288	4.1 ± 0.5	4.83 ± 0.01
$3d^6(a\,^3F)4p$	$x\,^4D^o$	7/2	62 945.04	2498.898	2.8 ± 0.3	
$3d^6(a\,^3F)4p$	$y\,^4G^o$	9/2	63 948.79	2430.078	2.7 ± 0.3	
$3d^6(a\,^3F)4p$	$y\,^4G^o$	7/2	64 040.89	2432.261	2.7 ± 0.3	

[a] Smith and Whaling (1973).

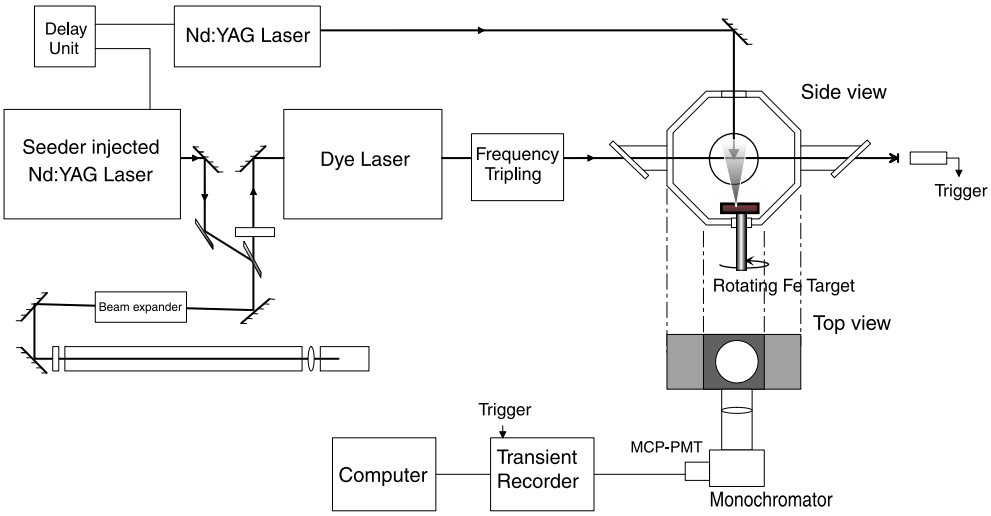

Figure 3. Experimental set-up.

power is thus increased since the loss in pulse energy is only a factor of two. A more detailed description of the SBS compressor can be found in Li *et al* (1999b).

The pulse from the SBS compressor was used to pump a Continuum ND 60 dye laser running on the dye DCM, providing tunable radiation in the region 615–660 nm. The laser radiation was frequency doubled in a KDP crystal and, after rotating the polarization direction in a retarding plate, mixed in a BBO crystal to obtain the third harmonic. The light from the dye laser thus provided excitation wavelengths between 205 and 220 nm. The bandwith of the UV radiation was approximately 2 pm.

The UV radiation crosses the expanding plasma cloud with a variable delay to the ablation laser. The two Nd:YAG lasers were internally triggered using a digital delay generator. The LIF was detected in a direction perpendicular to both the ablation and the excitation laser beam. The signal was focused onto the slit of a 0.2 m monochromator. LIF was detected in a strong decay channel, different from the excitation wavelength to decrease the influence of laser stray light. The LIF detection wavelength is given in table 1. A Hamamatsu 1564U microchannel-plate (MCP) photomultiplier, with a risetime of 200 ps, was used to detect the

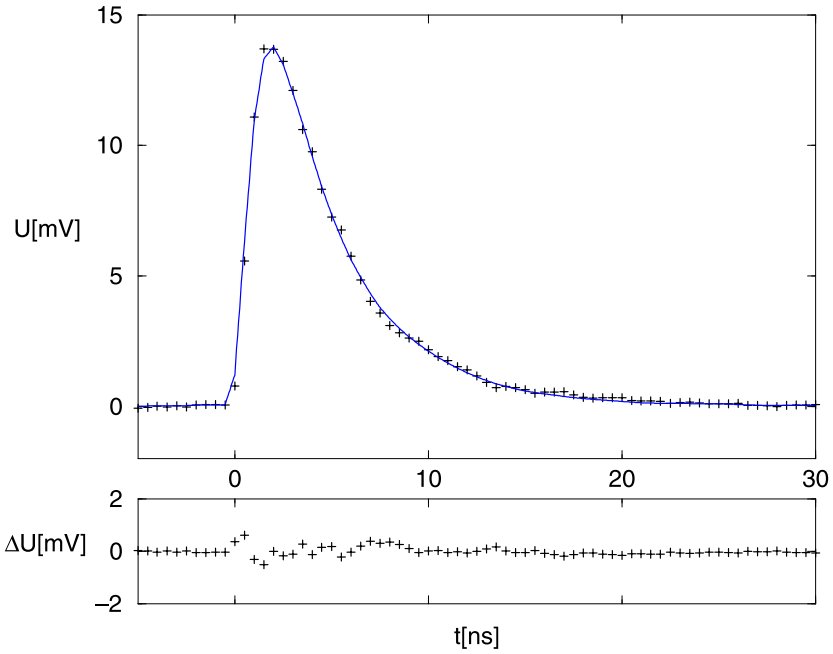

Figure 4. Figure of a measured and evaluated LIF for one of the levels. In the upper figure, the full curve shows the function fitted to the recorded data points, which are plotted as +. The residual (difference between the data points and the fitted function) is plotted below. The fitted function gives a lifetime of 3.32 ns.

LIF. The signal was recorded time-resolved using a Tektronix DSA 602 transient digitizer with an analogue bandwidth of 1 GHz and a real-time sampling rate of 2 GS/s. The data were transferred to a PC and analysed.

For all laser excitations, the lower level is the metastable $a^2G_{9/2}$ level of the $3d^7$ configuration at 15 844.65 cm^{-1}. Due to the relatively high energy of this metastable level, the excitation beam must interact with the plasma close to the ablation point, where the population of ions in metastable levels is sufficiently high. However, even though the LIF signal can be enhanced in this way, the plasma background is simultaneously increased. Much care was taken in adjusting the focus and intensity of the ablation laser as well as the position and delay of the excitation laser beam to achieve an optimal signal-to-noise ratio (SNR). In some measurements a non-negligible background from the plasma glow was subtracted before evaluation of the LIF. The influence of collisions in the plasma was checked to avoid systematic errors. This was done by recording lifetimes while varying the power and focus of the ablation laser, by changing the delay time between the ablation and excitation laser and by changing the position of the excitation beam in the plasma. The LIF was evaluated by fitting a convolution of an exponential decay and the recorded laser pulse to the measured LIF curve. An example of a LIF signal and the fitted function is given in figure 4. An average of 10–20 recordings were taken for each level and the average value is given as the lifetime. The error estimates reflect the spread in lifetime between different evaluations and include any possible systematic errors.

4. Measurements of branching fractions

The branching fractions (BFs) are obtained by measuring the calibrated intensity of as many lines (branches) as possible from a given upper energy level. The spectrum used for the intensity measurements were recorded at the Lund UV FTS. The instrument is optimized in the UV region, and can record spectra in the region 1850–7000 Å. However, it is not possible to record the whole region in one single experiment, due to the spectral response of available photomultipliers as well as the effect of aliasing. The FTS is an appropriate instrument for branching fraction measurements, since it is possible to record a reasonably wide wavelength region, while still retaining a high SNR.

The Fe II spectrum was recorded in the region 33 000–50 000 cm^{-1} (3000–2000 Å) using a hollow cathode lamp with a mixture of argon and neon as a carrier gas. The detector used was a Hamamatsu R166. The neon hollow cathode normally gives a rich Fe II spectrum due to the excitation by charge transfer (Johansson and Litzén 1978). However, the 4p levels studied in the present paper are located at too low energies to be effectively populated through charge transfer with neon. Collisions with argon ions should be more effective in exciting these 4p states due to the lower ionization potential of argon. In the hollow cathode spectrum we could measure the intensity for a total of seven lines from the two levels without strong branches below 1850 Å. A remarkable improvement was found when recording the spectrum with a Penning discharge lamp, run at a current of 1 A. The electronic excitation in the Penning discharge is more efficient than in the hollow cathode and the energy levels around 60 000 cm^{-1} are obviously more populated. The higher SNR in the Penning discharge spectrum made it possible to measure intensities for a total of 18 lines. Because of this, only the Penning spectrum was used for the intensity measurements.

The photometric calibration (the response function) of the instrument and the detectors is the largest source of uncertainties in the intensity measurements. It was done with the aid of a continuous light source with a known spectral intensity distribution. A deuterium lamp equipped with an MgF_2 window, calibrated to within 8% (two standard deviations (2σ)) in the interval 166–410 nm by Physikalisch-Technische Bundesanstalt, Berlin, Germany, provided a continuous reference spectrum in the region 33 000–60 000 cm^{-1}. Ar II lines with known branching fractions (Siems *et al* 1973) were used as an internal control, since the light emitted by Ar II and by Fe II travels an identical optical path. The agreement between the two calibration methods was within 10%.

The FTS produces an interferogram, which is the inverse Fourier transform of the spectrum. The recorded interferograms were transformed using the program GREMLIN, a development of the program DECOMP (Brault and Abrams 1989). The spectrum is assigned a linear wavenumber scale, good to within the stability and alignment of the HeNe laser used for sampling. The spectrum was intensity calibrated, by applying an average of the response function taken before and after the spectrum. A Voigt function was fitted to the individual lines, and the area under the fitted profile was used as the line intensity.

The largest intensity ratios we measured were between 200 and 400 for the two levels, respectively, giving a dynamic range of about three orders of magnitude of the branching fractions. The total intensity of the unobserved branches is estimated from comparisons with theoretical calculations to be of the order of 1%. By including these calculated intensities the branching fractions are derived for each transition originating from one of the two levels studied and included in table 2. Our experimental data are compared with the values calculated by Raassen and with measurements for one of the levels by Smith and Whaling (1973). There is an extremely good agreement between the two sets of measurements and a

Table 2. Absolute oscillator strengths of Fe II transitions.

Upper level	Lower level	λ (Å)[a]	σ (cm^{-1})	BF Expt	BF R[b]	BF SW[b]	log gf	Unc.[c] (%)
z ^{4}I$^o_{9/2}$	3d^7 a ^{2}G$_{9/2}$	2189.034	45 667.98	0.007	0.009		−1.850	17
	3d^7 a ^{2}H$_{11/2}$	2428.077	41 172.36	0.002	0.002		−2.207	18
	3d^6(^{3}H)4s a ^{4}H$_{11/2}$	2494.117	40 082.26	0.010	0.013		−1.557	17
	3d^6(^{3}H)4s a ^{4}H$_{9/2}$	2503.565	39 931.01	0.089	0.099		−0.624	16
	3d^6(^{3}H)4s a ^{4}H$_{7/2}$	2511.760	39 800.73	0.805	0.780		+0.338	9
	3d^6(^{3}F)4s b ^{4}F$_{9/2}$	2571.549	38 875.42	0.010	0.009		−1.542	17
	3d^6(^{3}F)4s b ^{4}F$_{7/2}$	2583.054	38 702.28	0.008	0.009		−1.665	17
	3d^6(^{3}G)4s a ^{4}G$_{11/2}$	2770.505	36 083.84	0.014	0.014		−1.328	17
	3d^6(^{3}G)4s a ^{4}G$_{7/2}$	2813.618	35 530.97	0.012	0.017		−1.394	17
	3d^6(^{3}H)4s b ^{2}H$_{11/2}$	2828.629	35 342.42	0.024	0.027		−1.081	17
	3d^6(^{3}H)4s b ^{2}H$_{9/2}$	2843.317	35 159.85	0.005	0.006		−1.770	19
Residual				0.013				
z ^{2}I$^o_{11/2}$	3d^7 a ^{2}H$_{9/2}$	2388.389	41 856.47	0.083	0.068	0.0670	−0.684	16
	3d^6(^{3}H)4s a ^{4}H$_{13/2}$	2414.102	41 410.69	0.004	0.004	0.0046	−1.958	17
	3d^6(^{3}H)4s a ^{4}H$_{9/2}$	2433.499	41 080.63	0.053	0.056	0.0438	−0.858	16
	3d^6(^{3}F)4s b ^{4}F$_{9/2}$	2497.684	40 025.03	0.003	0.003		−2.023	17
	3d^6(^{3}G)4s a ^{4}G$_{11/2}$	2684.961	37 233.43	0.003	0.003	0.0021	−2.084	19
	3d^6(^{3}G)4s a ^{4}G$_{9/2}$	2712.391	36 856.92	0.053	0.056	0.0509	−0.768	16
	3d^6(^{3}H)4s b ^{2}H$_{11/2}$	2739.516	36 492.00	Bl[d]	0.019			
	3d^6(^{3}H)4s b ^{2}H$_{9/2}$	2753.288	36 309.48	0.776	0.785	0.8275	+0.412	10
Residual				0.025				

[a] Wavelengths from Johansson (unpublished data).
[b] R, Raassen (this work); SW, Smith and Whaling (1973).
[c] Uncertainty in the f-value.
[d] Blended by a strong Fe II line.

remarkably good agreement between the measurements and the calculations, considering the complexity of the atomic structure. Raassen's calculated values are extracted from database at ftp://ftp.wins.uva.nl/pub/orth/iron/FeII.E1

5. Derivation of oscillator strengths

By combining the branching fractions with the radiative lifetimes, absolute transition probabilities have been derived. The results for the two Fe II levels z ^{4}I and z ^{2}I are presented in table 2. For each transition the upper and lower level designations are given together with the air wavelength and wavenumber. Since the BF is defined as the transition probability of a single transition divided by the sum of the transition probabilities of all transitions from a given upper level, the intensity of all branches must be determined in order to find the correct BF. In practice this is seldom possible, and in most cases not necessary. There are sometimes branches outside the wavelength region accessible with available techniques and instruments, and if they are strong they introduce a larger error in the results. Weak lines outside the accessible wavelength region or absent in the observed spectra do not add any significant uncertainty to the results. They can therefore be replaced by theoretical predictions of the transition probabilities. The sums of these lines are based on Raassen's calculations and given as the *residual* in table 2. The line at 2739.516 Å is masked by the strong Fe II line at 2739.548 Å which belongs to one of the strongest multiplets in Fe II.

By normalizing using the radiative lifetimes the branching fractions are converted to A-values, which are then transferred to log gf values and inserted in table 2. The uncertainties given for the f-values in the last column include the estimated errors in the BF and in the lifetime measurements. The uncertainty in the BF mainly arises from three independent sources: an uncertainty in the measured area due to the fitting of the individual lines, an uncertainty in the radiometic response of the deuterium lamp and an error when applying the calibrated lamp curve to obtain the instrument response. Errors from the fitting procedure have been found to mainly depend on the SNR. This uncertainty was estimated by means of a computer simulation, where a Gaussian curve is fitted to computer-generated line profiles, including different amounts of noise (Blom, private communication). By means of iteration, σ was calculated by the computer individually for each line from the FWHM, resolution and SNR. Two σ was taken as the fitting uncertainty. Due to the relatively high ion temperature in a Penning discharge, on the order of 3000 K (Kling 1997, Litzén and Kling 1998), Doppler broadening will be the dominant broadening effect, and the lines will have almost pure Gaussian profiles. At 3000 K, the expected linewidth of an Fe line is about 0.21 cm^{-1}. Typical linewidths for an Fe II line at 2500 Å are 0.18 cm^{-1} in the hollow cathode and 0.28 cm^{-1} in the Penning discharge. A 4% uncertainty was used as the error in the photometric calibration of the deuterium lamp. The uncertainty when applying the deuterium lamp response curve to

Table 3. Experimental and theoretical oscillator strengths for 18 Fe II lines.

		log gf							
λ (Å)	Transition	a	b	c	d	e	f	g	h
2189.034	a ^{2}G$_{9/2}$–z ^{4}I$^o_{9/2}$	−1.850	−1.753	−1.385					
2388.389	a ^{2}H$_{9/2}$–z ^{2}I$^o_{11/2}$	−0.684	−0.763	−0.650	−0.377	−0.289			−0.85
2414.102	a ^{4}H$_{13/2}$–z ^{2}I$^o_{11/2}$	−1.958	−1.972	−1.751					−2.01
2428.077	a ^{2}H$_{11/2}$–z ^{4}I$^o_{9/2}$	−2.207	−2.199	−1.895					
2433.499	a ^{4}H$_{9/2}$–z ^{2}I$^o_{11/2}$	−0.858	−0.833	−0.843		−0.824	−0.72		−1.02
2494.117	a ^{4}H$_{11/2}$–z ^{4}I$^o_{9/2}$	−1.557	−1.446	−0.992	−2.627	−0.921	−1.35		
2497.684	b ^{4}F$_{9/2}$–z ^{2}I$^o_{11/2}$	−2.023	−2.058	−1.804					
2503.565	a ^{4}H$_{9/2}$–z ^{4}I$^o_{9/2}$	−0.624	−0.576	−0.497	−0.812	−0.548	−0.55		
2511.760	a ^{4}H$_{7/2}$–z ^{4}I$^o_{9/2}$	+0.338	+0.324	+0.306	+0.432	+0.316	+0.23		
2571.549	b ^{4}F$_{9/2}$–z ^{4}I$^o_{9/2}$	−1.542	−1.573	−1.580					
2583.054	b ^{4}F$_{7/2}$–z ^{4}I$^o_{9/2}$	−1.665	−1.592	−1.660					
2684.961	a ^{4}G$_{11/2}$–z ^{2}I$^o_{11/2}$	−2.084	−1.965	−1.900					−2.25
2712.391	a ^{4}G$_{9/2}$–z ^{2}I$^o_{11/2}$	−0.768	−0.736	−0.760		−1.149	<-0.21	−0.52	−0.86
2739.516	b ^{2}G$_{11/2}$–z ^{2}I$^o_{11/2}$		−1.208	−1.131	−1.611	−1.027			
2753.288	b ^{2}H$_{9/2}$–z ^{2}I$^o_{11/2}$	+0.412	+0.423	+0.210	+0.199	+0.520	+0.51	+0.45	+0.37
2770.505	a ^{4}G$_{11/2}$–z ^{4}I$^o_{9/2}$	−1.328	−1.322	−1.273		−1.495			
2813.618	a ^{4}G$_{7/2}$–z ^{4}I$^o_{9/2}$	−1.394	−1.242	−1.390		−1.018		−1.15	
2828.629	b ^{2}H$_{11/2}$–z ^{4}I$^o_{9/2}$	−1.081	−1.032	−0.836		−0.785			
2843.317	b ^{2}H$_{9/2}$–z ^{4}I$^o_{9/2}$	−1.770	−1.656	−1.750					

[a] This work; experimental.
[b] This work; theory.
[c] Kurucz (1993).
[d] Nahar (1995) (The IRON project).
[e] Fawcett (1987).
[f] Ekberg and Feldman (1992).
[g] Moity (1983).
[h] Smith and Whaling (1973).

determine the instrument response was estimated to be 10%. These three uncertainties and the uncertainty in the lifetime (see table 1) were added using the propagation of error formula to give the individual uncertainty in the f-value for each line.

6. Results and discussion

In table 3 we present a list of the measured Fe II lines sorted by wavelength. The experimental log gf values of table 2 are compared with observational and theoretical data available in the literature. The columns marked b–e contain theoretical data from Raassen (this work), Kurucz (1993), Nahar (1995) and Fawcett (1987), respectively. Column f are data derived from Fe II emission lines in the spectrum of the solar chromosphere (Ekberg and Feldman 1992), and column g gives laboratory arc measurements by Moity (1983). The last column (h) gives the log gf values by Smith and Whaling (1973) based on beam–foil lifetime measurements and the branching fractions included in table 2. The theoretical data are based on various codes: the Kurucz and Fawcett calculations utilize Cowan's code (1981), whereas Raassen's calculations are based on the orthogonal operator technique (Raassen and Uylings 1998a, b). Nahar's data are produced within the IRON project and are based on the R-matrix method (Nahar 1994), including the fine structure according to the LS recipe. In figures 5 and 6 we have compared our data with the theoretical data which show good agreement with our experimental values. Our values are compared with the values calculated by Raassen (b) and Kurucz (c) by plotting $\Delta\log gf$ against log gf. Raassen and Kurucz give log gf values for all the measured lines and allow a full comparison.

There is remarkably good agreement between Raassen's data and the experimental values, even for the weak 'intercombination lines'. The largest discrepancy is 0.15 on the logarithmic

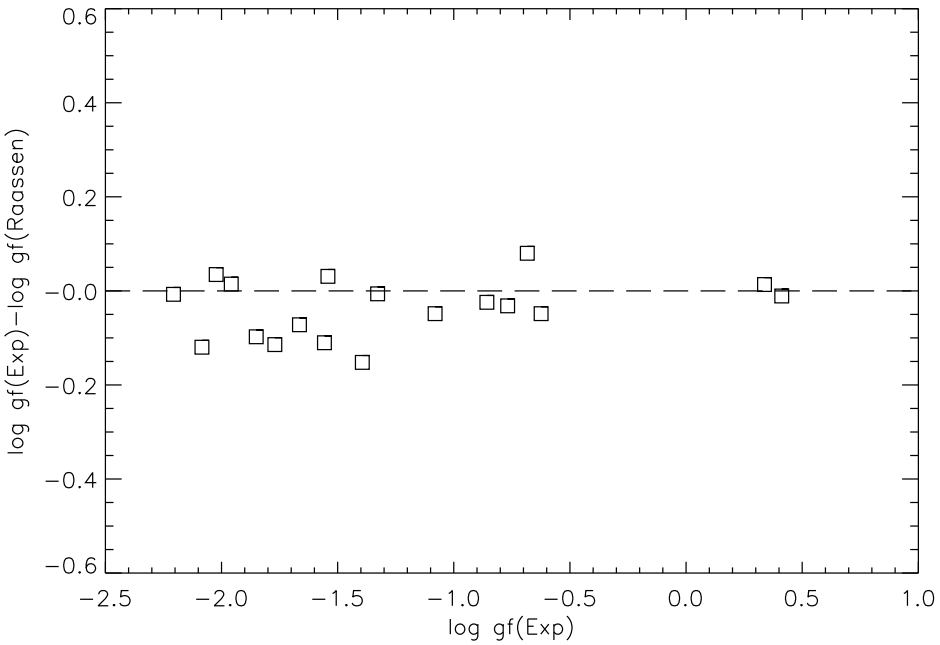

Figure 5. Comparison of our experimental f-values with theoretical data calculated by Raassen, by plotting $\Delta\log gf$ against log gf.

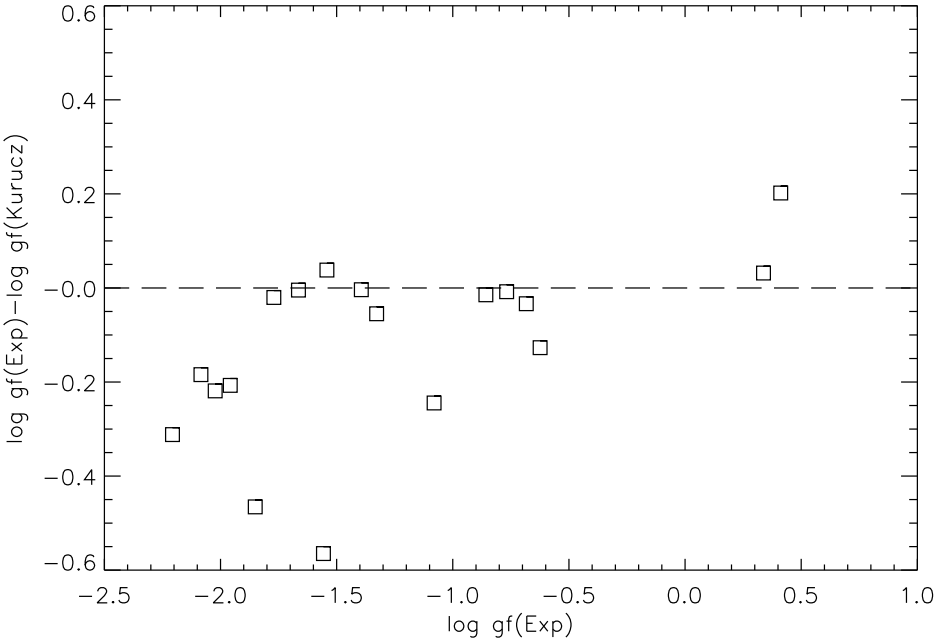

Figure 6. Comparison of our experimental f-values with theoretical data calculated by Kurucz, by plotting $\Delta\log gf$ against $\log gf$.

scale, corresponding to 41%, and the average discrepancy is 0.055 (14%). The differences are larger when comparing with Kurucz's data, and one of the largest discrepancies occurs for the strongest line, 2753 Å. Of the six LS allowed lines included in the IRON project data (d) one of them (2494 Å) differs by more than one order of magnitude. It is noteworthy that this line is also the most deviating line in Kurucz's database, where it differs by a factor of 3.7 in the opposite direction. Fawcett's value for this line is close to the Kurucz value, which might be expected as they have both used Cowan's code. However, for other lines there are big discrepancies between Fawcett's and Kurucz's values.

The solar data by Ekberg and Feldman contain six of the studied lines, and for one of these they give an upper limit. Four of the six lines give, in general, 0.1–0.2 too small values on the logarithmic scale, whereas the strongest line is 0.1 too strong. The solar data are obtained by reducing and analysing photographic recordings of the chromospheric spectrum of the sun, recorded by *Skylab*. Finally, the arc measurements by Moity only include three of the lines, the strongest of them being very close to the value presented in this paper.

7. Conclusions

We report experimental lifetimes for six medium excited Fe II levels, belonging to the subconfigurations $3d^6(^3H)4p$ and $3d^6(^3F)4p$. This is the first time that such high states have been measured using the LIF technique. For two of these levels, $z\,^4I_{9/2}$ and $z\,^2I_{11/2}$, we report experimental $\log gf$ values for 18 lines. All the lines appear in the 2000–3000 Å region. In a comparison with theoretical work we conclude that the calculations by Raassen using the orthogonal operator technique (Raassen and Uylings 1998a, b) produce values that in most cases differ by less than our quoted errors. It is too early to conclude that the whole spectrum

can be calculated with the same accuracy. As the level density increases with excitation energy, more configuration interactions and level mixing occur. We will continue measuring at higher excitation energies and compare with Raassen's calculations.

Acknowledgments

This project is financially supported by the TMR Programme 'Access to Large Scale Facilities', contract no ERBFMGECT950020(DG12), the Swedish Natural Science Research Council and the Swedish National Space Board. The authors would like to thank Dr Ulf Litzén for valuable advice and guidance during the FTS part of this work, and Mr Anders Blom for writing the computer program used in the uncertainty calculation. The excellent research conditions at Lund Laser Centre and the support by Professor S Svanberg are gratefully acknowledged.

References

Brandt J C *et al* 1999 *Astron. J.* **117** 1505
Brault J W and Abrams M C 1999 *High Resolution Fourier Transform Spectroscopy (OSA Technical Digest Series vol 6)* (Washington: Optical Society of America) p 110
Cowan R D 1981 *The Theory of Atomic Structure and Spectra* (Berkeley, CA: University of California Press)
Ekberg J O and Feldman U 1992 *Astrophys. J. Suppl.* **86** 611
Fawcett B C 1987 *At. Data Nucl. Data* **37** 333
Johansson S and Litzén U 1978 *J. Phys. B: At. Mol. Phys.* **11** L703
Kling R 1997 Entwicklung und Untersuchung einer Penningentladung zur Erzuegung von XUV Strahlung und als spektroskopische Lichtquelle höher ionisierter Spezies *PhD Thesis* Universität Hannover
Kurucz R L 1993 *SYNTHE Synthesis Programs and Line Data* Kurucz CD-ROM no 18
Leckrone D S, Proffitt C R, Wahlgren G M, Johansson S G and Brage T 1999 *Astron. J.* **117** 1454
Li Z-S, Lundberg H, Sikström C M and Johansson S 1999a *Eur. Phys. J.* D **6** 9
Li Z-S, Norin J, Persson A, Wahlström C-G, Svanberg S, Doidge P S and Biémont E 1999b *Phys. Rev.* A **60** 198
Litzén U and Kling R 1998 *J. Phys. B: At. Mol. Phys.* **31** L933
Moity J 1983 *Astron. Astrophys. Suppl.* **52** 37
Nahar S N 1995 *Astron. Astrophys.* **293** 967
Raassen A J J and Uylings P H M 1998a *Astron. Astrophys.* **340** 300
——1998b *J. Phys. B: At. Mol. Opt. Phys.* **31** 3137
Schnabel R, Kock M and Holweger H 1999 *Astron. Astrophys.* **342** 610
Siems A, Knauer J P, Kock M, Johansson S and Litzén U 1996 *J. Quant. Spectrosc. Radiat. Transfer* **56** 513
Smith P L and Whaling W 1973 *Astrophys. J.* **183** 313
Verner E M, Verner D A, Korista K T, Ferguson J W, Hamann F and Ferland G J 1999 *Astrophys. J. Suppl.* **120** 101